1 Introduction

Feedback

& Maler, 1999), which combines

Glass, 1997). Plant (1981) was a pioneer in this area, analyzing the dynamics of the FitzHugh-Nagumo neuron model with delayed positive or negative self-feedback. More recently, Giannakopoulos and Zapp (2001) considered one inhibitory and one excitatory neuron, coupled to each other and themselves, with delay; from the point of view of the excitatory neuron, this loop provides delayed inhibitory feedback. There have also been analyses of delay-induced oscillations and frustrations in neural nets with delays (Belair, Campbell, & van den Driessche, 1996), as well as of multistability in nets with single delays (Foss, Longtin, Mensour, & Milton, 1996), multiple delays (Shayer & Campbell, 2000) or multiple loops (Campbell 1999; Glass & Malta, 1990). Traveling waves in pulse-coupled integrate-and-□re neurons with delays have been found by Bressloff and Coombes (1999). The same authors have also found that rhythmic bursting patterns can occur in asymmetric networks of linear integrate-and-□re neurons with additive synaptic inputs (i.e., without reversal potentials), when there was a mixture of inhibitory and excitatory synaptic coupling (Bressloff & Coombes, 2000a).

Despite all these studies, delayed paired feedback, especially in the presence of noise, has not received much attention from the dynamical point of view, even though it is frequently encountered (Crick & Koch, 1998; Murphy et al., 1999; Berman & Maler, 1999; Hahnloser et al., 2000). Here we combine both delayed feedback with the ability to change independently the strengths of the excitatory and inhibitory components of the feedback in the context of a neuron embedded in a network. These feedbacks can have different properties, such as different strengths, integration and synaptic timescales, and propagation delays. Recurrent excitation and inhibition, and as we will see under certain conditions, mixed feedback are special cases of this paired feedback.

Our article provides a general framework for analyzing paired feedback with delays and noise due, for example, to synaptic activity. It reveals that as a whole, the paired feedback loop forms a sophisticated computational unit in comparison with a single neuron due to the wide variety of □

model for the simplest

between the loops (i.e., their relative strengths), regardless of the cause of this balance, and as a function of the input (nonfeedback) bias current.

The neuron model we use at the core of the feedback loop is a leaky integrate–and–fire neuron with reversal potentials whose governing equation is

$$C\frac{dV}{dt} = I - g_L(V_L - V) - g_e(V_e - V) - g_i(V_i - V) \tag{2.1}$$

with reset and threshold values V_r and V_μ, respectively; that is, if $V(t^-) = V_\mu$, then $V(t^+) = V_r$. C is the capacitance, I is the input current, and g_L, g_e, and g_i are the leak, excitatory, and inhibitory conductances, respectively. V_L is the leak potential, and V_e and V_i are the excitatory and inhibitory reversal potentials, respectively. We assume that there is an absolute refractory period τ_r—that $V = V_r$ for a time τ_r after each firing. The instantaneous firing rate of model 2.1 is

$$f(t) = H(V_{ss}(t) - V_\mu)\left[\tau_r - \frac{C}{g_{tot}(t)}\ln\left(\frac{V_\mu - V_{ss}(t)}{V_r - V_{ss}(t)}\right)\right]^{-1}, \tag{2.2}$$

where H is the Heaviside function,

$$g_{tot}(t) = g_L + g_e(t) + g_i(t) \tag{2.3}$$

and

$$g_{tot}(t)V_{ss}(t) = g_L V_L + g_e(t)V_e + g_i(t)V_i + I. \tag{2.4}$$

This approximation for the firing rate is due to the fact that an equality in equation 2.2 is appropriate only if all quantities in equation 2.1 are constant (apart from the voltage). Here, however, we assume that the conductances g_e and g_i are functions of time, since they are affected by feedback activity (see below). This activity is also assumed to vary on a timescale slower than the membrane time constant in the leaky integrate-and-fire (LIF) model. The timescale of the feedback activity is a function of both the response properties of the population 2 cells (Pd

To implement feedback in the model, equation 2.1, we assume that the excitatory and inhibitory conductances depend on the firing frequency of the neuron at times in the past. Specifically, we write g_e and g_i as

$$g_e(t) = \bar{g}_e \int_{t-\tau_e}^{\infty} G_e^{m_e}(t-s) f(s)\, ds \tag{2.5}$$

$$g_i(t) = \bar{g}_i \int_{t-\tau_i}^{\infty} G_i^{m_i}(t-s) f(s)\, ds; \tag{2.6}$$

where the feedback kernels G_e and G_i are described below. We are assuming here a homogeneous population of neurons that communicate mainly via feedback (directly or via another population), and the firing function $f(t)$ drives this feedback activity. This function f can be seen as the population instantaneous rate under asynchronous conditions, obtained by summing all spike trains from all the cells. Since all cells are identical as a first approximation, they all receive the same time-dependent synaptic input, and each of their behaviors is governed by equations 2.5 and 2.6 in conjunction with equation 2.2. The feedback gains $\bar{g}_e, \bar{g}_i$ account among other things for the number of neurons summing their output. The firing frequency, equation 2.2, is thus a good approximation to the population instantaneous rate for slowly varying inputs.

The feedback kernels are chosen as

$$G_e^{m_e}(t) = \begin{cases} \frac{a_e^{m_e+1}}{m_e!}(t-\tau_e)^{m_e} \exp[-a_e(t-\tau_e)] & \text{if } \tau_e < t \\ 0 & \text{if } \tau_e > t \end{cases} \tag{2.7}$$

and

$$G_i^{m_i}(t) = \begin{cases} \frac{a_i^{m_i+1}}{m_i!}(t-\tau_i)^{m_i} \exp[-a_i(t-\tau_i)] & \text{if } \tau_i < t \\ 0 & \text{if } \tau_i > t. \end{cases} \tag{2.8}$$

The function $G_e^{m_e}(t)$ is zero until time τ_e, after which it rises to a maximum before decaying back to zero from above. τ_e (and also τ_i below) represents the minimal delay for activity to propagate around the loop. This value can be set to zero in our formalism, as is often done in modeling neural circuitry and neural networks, but our analysis is valid for any (zero or positive) τ_e and τ_i. Note that the total mean delay is $\tau_{e;i} + (m_{e;i}+1)/a_{e;i}$. Thus, $g_e(t)$ is a scaled convolution of the firing frequency $f(t)$ in the past with the convolution kernel $G_e^{m_e}(t)$. This convolution smoothes $f(t)$ and is meant to mimic the effect of the output of the neuron exciting another cell or collection of cells, which then project back in a paired fashion to the neuron under study. Note that $g_e(t)$ depends on f only at times earlier than $t - \tau_e$. Similar statements hold for $g_i(t)$. The coefficients $\bar{g}_e$ and $\bar{g}_i$ are the nonnegative strengths of the excitatory and inhibitory feedback, respectively. In practical situations, τ_i is

if $m_e > 1$. This process can be repeated for y_{m_e-2} and so on, and terminates when $m_e = 1$. In this case, we have

$$y_0(t) = \int_{t-\tau_e}^{t} a_e \exp[-a_e(t-s-\tau_e)] f(s)\, ds; \tag{2.17}$$

so that

$$\frac{dy_0}{dt} = -a_e \int_{t-\tau_e}^{t} a_e \exp[-a_e(t-s-\tau_e)] f(s)\, ds + a_e f(t-\tau_e) = a_e[f(t-\tau_e) - y_0(t)]. \tag{2.18}$$

Thus, combining equations 2.13 and 2.16 for $m_e > 1$ and equation 2.18, we have $m_e + 1$ equations:

$$\frac{dg_e}{dt} = a_e[\bar{}_e y_{m_e-1} - g_e] \tag{2.19}$$

$$\frac{dy_{m_e-1}}{dt} = a_e[y_{m_e-2} - y_{m_e-1}] \tag{2.20}$$

$$\vdots$$

$$\frac{dy_1}{dt} = a_e[y_0 - y_1] \tag{2.21}$$

$$\frac{dy_0}{dt} = a_e[f(t-\tau_e) - y_0]; \tag{2.22}$$

where, if not indicated, the variables on the right-hand sides are evaluated at time t. A similar process can be undertaken for g_i, resulting in a further $m_i + 1$ equations:

$$\frac{dg_i}{dt} = a_i[\bar{}_i z_{m_i-1} - g_i] \tag{2.23}$$

$$\frac{dz_{m_i-1}}{dt} = a_i[z_{m_i-2} - z_{m_i-1}] \tag{2.24}$$

$$\vdots$$

$$\frac{dz_1}{dt} = a_i[z_0 - z_1] \tag{2.25}$$

$$\frac{dz_0}{dt} = a_i[f(t-\tau_i) - z_0]. \tag{2.26}$$

Equations 2.5 and 2.6 are integral equations relating the conductances $g_e(t)$ and $g_i(t)$ to $f(t)$. Because of the form of $G_e^{m_e}$ and $G_i^{m_i}$, we have been able to derive a set of equivalent delay differential equations that govern the dynamics of $g_e(t)$ and $g_i(t)$. Recalling that $f(t)$ is a function of $g_e(t)$ and $g_i(t)$

through equation 2.2, equations 2.19 through 2.26 form a closed system. They will be a valid description of the dynamics of equations 2.1, 2.5, and 2.6, provided the spiking dynamics of the neuron occur on a fast timescale relative to the timescale of the feedback delay and of the time evolution of the conductances associated with the feedback activity.

One way to think of equations 2.19 through 2.22 is that y_0 is a low–pass filtered version of $f(t - \tau_e)$, y_i is a low–pass filtered version of y_{i-1} for $i = 1, \ldots, m_e - 1$, and g_e is a low–pass filtered version of y_{m_e-1}, with strength $\bar{}_e$. The delayed quantity $g_e(t - \tau_e)$ is then used in determining $f(t - \tau_e)$ via equations 2.2 and 2.4. Equations 2.23 through 2.26 can be interpreted in a similar way. We now

Note that the □xed points

$$D \frac{\bar{e}}{i}[\bar{}_i f.g_e.t\ i\ ¿/; g_i.t\ i\ ¿//\ i\ g_i.t/] \tag{4.6}$$

$$D \bar{}_e f.g_e.t\ i\ ¿/; g_i.t\ i\ ¿//\ i\ g_e.t/; \tag{4.7}$$

which is just equation 4.2. Thus when $\bar{}_i$ D 0, the attractor of the system 4.2 and 4.3 with paired feedback lies on the line g_e D $\bar{}_e g_i = \bar{}_i$ and is governed by the single delay differential equation,

$$\frac{dg_i.t/}{dt} D \bar{}_i f.\bar{}_e g_i.t\ i\ ¿/=\bar{}_i; g_i.t\ i\ ¿//\ i\ g_i.t/: \tag{4.8}$$

If $\bar{}_i$ D 0, we have the single equation,

$$dg_e\bar{}$$

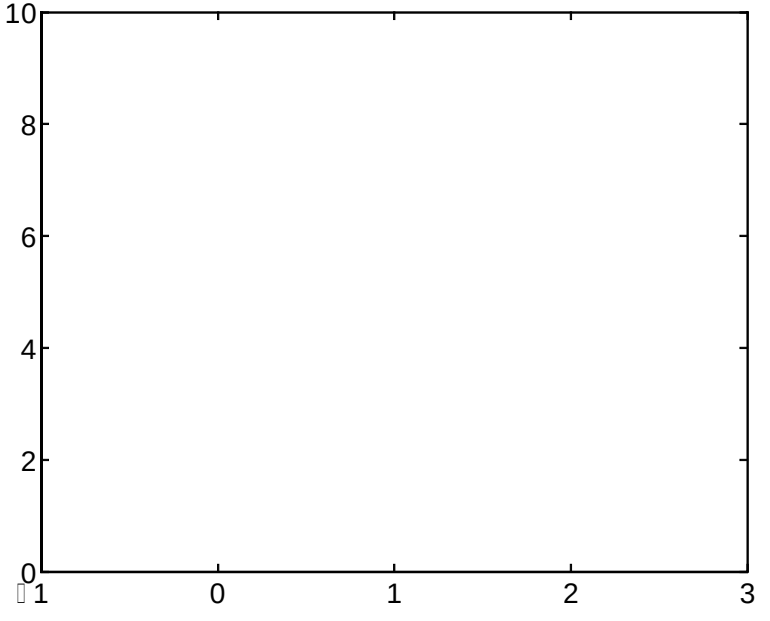
10
8
6
4
2
0
1
0
1
2
3

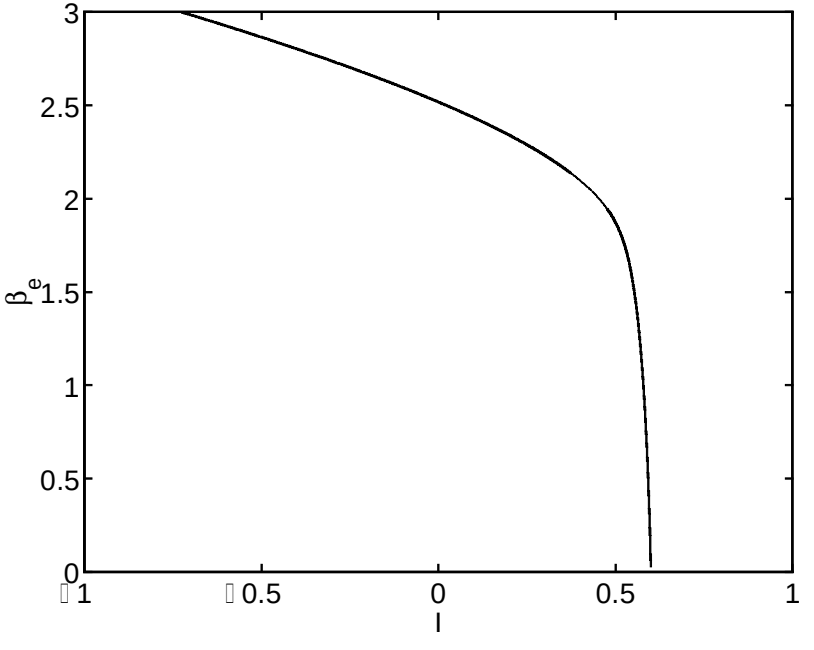

Figure 2: The curve of saddle-node bifurcations of □

then all roots of equation 4.12 have negative real part, and the fixed point g_0 of equation 4.9 is asymptotically stable.

By plotting $\bar{\epsilon}_e f(g, 0)$ as a function of g for various values

of A at which pairs of roots of the characteristic equation 4.16 cross the imaginary axis and acquire a positive real part. The crossing of the first such pair brings on a Hopf bifurcation; the subsequent crossing of the other pairs alters the shape of the oscillation of the firing frequency: the closer the real parts of the root pairs are, the more the oscillation resembles a square wave. Similar behavior is seen in singularly perturbed delay-differential equations (see, e.g., Mensour & Longtin, 1998). Accordingly, such solutions can be qualified as bursting, since spikes occur in clusters separated by periods of quiescence. It is important to realize that such bursting solutions are due to the network, that is, to the feedback loop, since the core integrate-and-fire neuron with reversal potentials cannot burst autonomously. If, for large enough I, $-1 < A < 0$, the fixed point of equation 4.15 will be stable, and as I is decreased, it will lose stability through the first of the Hopf bifurcations.

To study Hopf bifurcations in equation 4.14, we substitute $\lambda = i\omega$ into equation 4.12, separate real and imaginary parts, and obtain the two equations

$$A\cos(\omega - \phi) = 1 \tag{4.17}$$

and

$$A\sin(\omega - \phi) = -\omega. \tag{4.18}$$

Note that for equation 4.17 to be satisfied, we require $1 \le |A|$.

From equations 4.17 and 4.18, we have that

$$\phi = \frac{\cos^{-1}(1/A) + 2n\pi}{\sqrt{A^2 - 1}} \tag{4.19}$$

at a Hopf bifurcation for some nonnegative integer n, and the frequency of oscillation (at the bifurcation) is given by $\omega = \sqrt{A^2 - 1}$. We claim that for a fixed $0 < \phi$ and any $n \in \{0, 1, 2, \ldots\}$, there is an $A \in (-1, -1)$ such that equation 4.19 is satisfied. To see this, note that equations 4.17 and 4.18 imply that $\cos^{-1}(1/A) \in (\pi/2, \pi)$. Thus,

the maximum frequency during one oscillation tends to zero as I tends to I_c from above and that this curve has infinite slope at $I = I_c$. The actual frequency of oscillations in g_i also tends to zero as I tends to I_c from above, and simulations suggest that the period of oscillation scales as $-\log(I - I_c)$ as I tends to I_c from above (not shown). Both of these results are due to the nonsmoothness of the firing function f at $I = I_c$.

We note as well that the range of input current values over which the unstable fixed point occurs (the dashed line in Figure

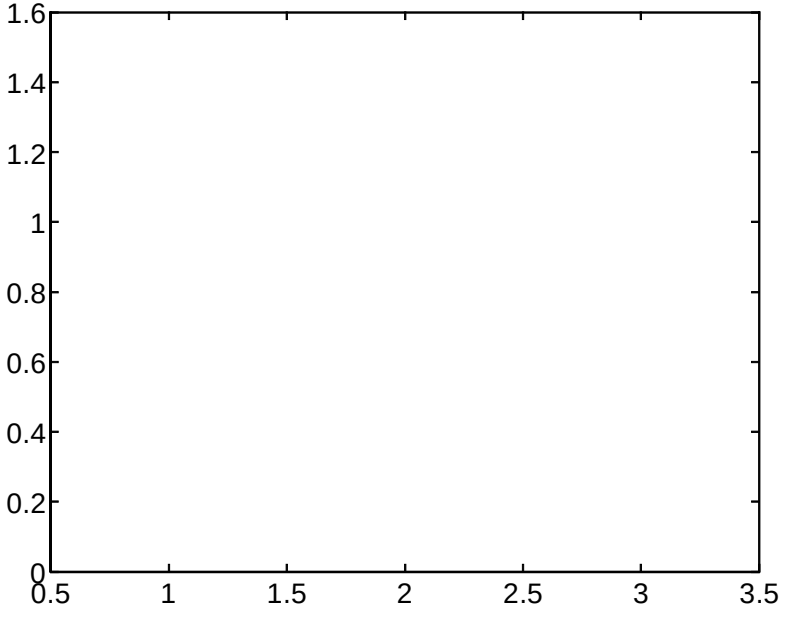
1.6
1.4
1.2
1
0.8
0.6
0.4
0.2
0
0.5
1
1.5
2
2.5
3
3.5

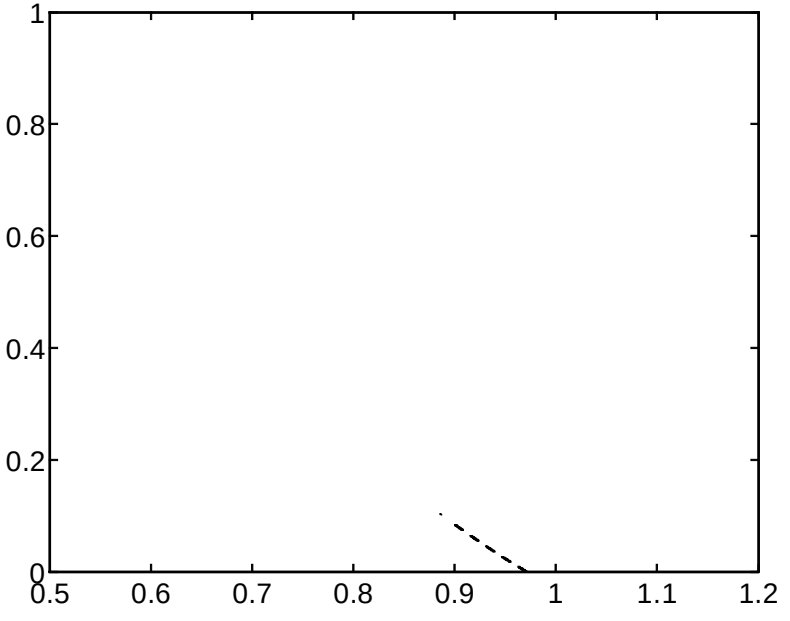
1
0.8
0.6
0.4
0.2
0
0.5
0.6
0.7
0.8
0.9
1
1.1
1.2

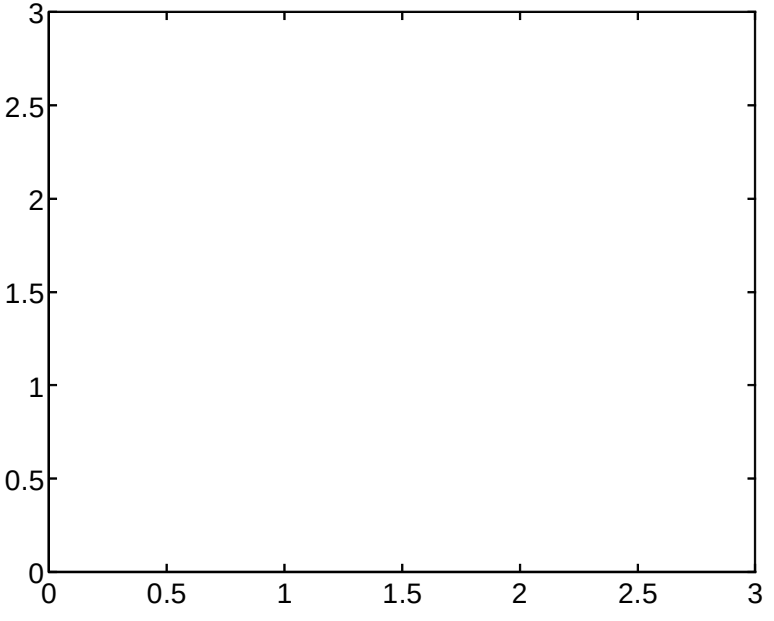
3
2.5
2
1.5
1
0.5
0
0
0.5
1
1.5
2
2.5
3

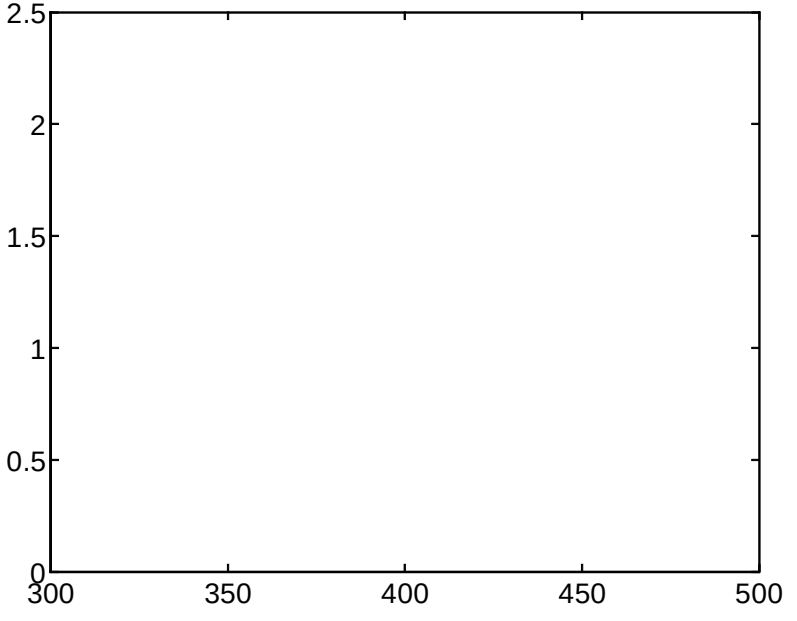
2.5
2
1.5
1
0.5
0
300
350
400
450
500

Now the right-hand side (r.h.s.) of equation 5.7 is negative except when s is zero, and thus trajectories approach the manifold on which $s = 0$. By considering the time evolution of $(z_0 - y_0)$ and of $(g_e - \bar{g}_e g_i/\bar{g}_i)$ from equation 5.1 through 5.4, it is clear that the manifold is invariant.

Note that if either $\bar{g}_e$ or $\bar{g}_i$ is zero, we only need consider half of the variables.

The linearization of equations 5.5 and 5.6 about a fixed point is

$$\frac{dx_1}{dt} = -\bar{g}_i x_2 - x_1 \tag{5.8}$$

$$\frac{dx_2}{dt} = [\bar{g}_e d_1/\bar{g}_i + d_2]x_1/(\tau - \tau_i) - x_2; \tag{5.9}$$

where $d_{1,2}$ is the derivative of f with respect to its first/second argument, evaluated at the fixed point. Looking for solutions of the form $[x_1\ x_2]^T = Be^{\lambda t}$, where $B \in \mathbf{R}^2$ and x^T denotes the transpose of x, we find that λ satisfies

$$\lambda^2 + 2\lambda + 1 - (\bar{g}_e d_1 + \bar{g}_i d_2/e^{\lambda\tau})/\tau = 0. \tag{5.10}$$

Note that this equation is still valid even if $\bar{g}_i = 0$, as an analysis of equations 5.1 through 5.4 shows. Equations such as 5.10 arise in the analysis of linear oscillators with delayed feedback (Campbell, 1999; Stepán 1989).

Defining $A \equiv \bar{g}_e d_1 + \bar{g}_i d_2$, we have a theorem regarding the roots of equation 5.10:

Theorem 2. If either $-1 < A < 1$, or $A < -1$ and

$$\tau < \frac{\cos^{-1}[(2 + A)/(-A)]}{\sqrt{-A - 1}}; \tag{5.11}$$

then all roots of equation 5.10 have negative real part.

Proof. When $A = 0$, the only roots of equation 5.10 are $\lambda = -1$, so the corresponding fixed point of equations 5.5 and 5.6 is stable. The only way the fixed point can become unstable is by λ crossing the imaginary axis. Substituting $\lambda = i\omega$ into equation 5.10, where ω is real, we have the equations

$$A\cos(\omega\tau) = 1 - \omega^2 \tag{5.12}$$

$$A\sin(\omega\tau) = -2\omega: \tag{5.13}$$

By squaring equations 5.12 and 5.13 and then adding them together, we obtain

$$A^2 = (1 + \omega^2)^2: \tag{5.14}$$

$$\frac{dz_0}{dt} D f.0; g_i.t ¡ ¿// ¡ z_0: \tag{5.19}$$

As argued in section 5.1, the fixed points are the same as for the m D 0 case; for each value of I, there is only one fixed point. Also, A < 0 if we are above the firing threshold, and so there cannot be any bifurcations at which ¸ D 0. If A < ¡1, it is possible to have a Hopf bifurcation. In fact, there is an infinite number of Hopf bifurcations as I decreases, just as there was for m D 0, although the conditions for bifurcation are not the same.

Recall that at a Hopf bifurcation,

$$¿ D \frac{\cos^{i\,1}[.2 C A/=A] C 2n¼}{p\overline{¡A ¡ 1}} \tag{5.20}$$

for some nonnegative integer n.

fixed amounts to a sharper localization in time of the delayed feedback. The case $m \to \infty$ corresponds to a delta function delay kernel. As in the cases $m = 0, 1$, we have a theorem regarding the existence of an attracting invariant manifold:

Theorem 3. If $1 < m$ and neither $\bar{\tau}_e$ nor $\bar{\tau}_i$ are zero, then there is an attracting invariant manifold on which

$$[g_e, y_{m-1}, \ldots, y_0, g_i, z_{m-1}, \ldots, z_0] = [\bar{\tau}_e g_i/\bar{\tau}_i, z_{m-1}, \ldots, z_0, g_i, z_{m-1}, \ldots, z_0] \tag{6.1}$$

that is, the excitatory dynamics are slaved to the inhibitory ones (assuming that $\bar{\tau}_i \neq 0$).

Proof. Similarly to theorem 1, define

$$s = (1/\bar{\tau}_e^2)(g_e - \bar{\tau}_e g_i/\bar{\tau}_i)^2 + \sum_{i=0}^{m-1} (y_i - z_i)^2.$$

We have

$$\frac{ds}{dt} = (2/\bar{\tau}_e^2)(g_e - \bar{\tau}_e g_i/\bar{\tau}_i)[(\bar{\tau}_e/\bar{\tau}_{m-1})(y_{m-1} - z_{m-1}) + (g_e - \bar{\tau}_e g_i/\bar{\tau}_i)] \tag{6.2}$$

$$- 2\sum_{i=0}^{m-1} (y_i - z_i)^2 + 2\sum_{i=1}^{m-1} (y_i - z_i)(y_{i-1} - z_{i-1}); \tag{6.3}$$

which can be rewritten as

$$\frac{ds}{dt} = -(2/\bar{\tau}_e^2)(g_e - \bar{\tau}_e g_i/\bar{\tau}_i)^2 + (2/\bar{\tau}_e)(y_{m-1} - z_{m-1})(g_e - \bar{\tau}_e g_i/\bar{\tau}_i) - (y_{m-1} - z_{m-1})^2 \tag{6.4}$$

$$- \sum_{i=2}^{m-1} [(y_i - z_i)^2 - 2(y_i - z_i)(y_{i-1} - z_{i-1}) + (y_{i-1} - z_{i-1})^2] \tag{6.5}$$

$$- [(y_1 - z_1)^2 - 2(y_1 - z_1)(y_0 - z_0) + 2(y_0 - z_0)^2]. \tag{6.6}$$

Since $0 < \bar{\tau}_e$, the right-hand side of equation 6.4 is negative when $s \neq 0$ and zero otherwise. All terms within the square brackets in equation 6.5 are either positive or zero, and the term within the square brackets in equation 6.6 is posi

The excitatory dynamics are slaved to the inhibitory ones, whose dynamics are given by

$$\frac{dg_i}{dt} = \bar{}_i z_{m\,i\,1} \;i\; g_i \tag{6.7}$$

$$\frac{dz_{m\,i\,1}}{dt} = z_{m\,i\,2} \;i\; z_{m\,i\,1} \tag{6.8}$$

$$\vdots \tag{6.9}$$

$$\frac{dz_1}{dt} = z_0 \;i\; z_1 \tag{6.10}$$

$$\frac{dz_0}{dt} = f.\bar{}_e g_i.t \;¡\; ¿/=\bar{}_i; g_i.t \;¡\; ¿// \;¡\; z_0; \tag{6.11}$$

where, if an argument is not given, the quantity is evaluated at time t. Performing the usual stability analysis, we □nd that if ¸ is an eigenvalue associated with the linearization of equations 6.7 through 6.11 about a □xed point, the determinant of the following matrix must be zero:

$$B \acute{} \begin{matrix} 0 \\ \\ \\ \\ \\ @ \end{matrix} \begin{matrix} ¸ C 1 & i \bar{}_i & 0 & ¢¢¢ & ¢¢¢ & 0 \\ 0 & & & & & \end{matrix}$$

Table 2: Bifurcation Conditions on ¿ and A.

m	$!^2$	¿
0	$A^2 ¡ 1$	$f_0^n.A/ ´ \cos^{¡1}.1=A/ C 2n¼g= \sqrt{A^2 ¡ 1}$
1	$¡A ¡ 1$	$f_1^n.A/ ´ \cos^{¡1}[.2 C A/=A] C 2n¼g= \sqrt{¡A ¡ 1}$
2	$\sqrt{A^2 ¡ 1}$	$f_2^n.A/ ´ \cos^{¡1}[.4 ¡ 3\sqrt{A^2}/=A] C 2n¼g= \sqrt{\sqrt{A^2 ¡ 1}}$
3	$\sqrt{¡A ¡ 1}$	$f_3^n.A/ ´ \cos^{¡1}[.8 ¡ 8\sqrt{¡A} ¡ A/=A] C 2n¼g= \sqrt{\sqrt{¡A ¡ 1}}$

We can see that the only way the □xed point can lose stability as A is decreased from 0 is through a Hopf bifurcation, and that this can occur only for $A < ¡1$. Setting $¸ D i!$ in equation 6.12 and separating the real and imaginary parts, we obtain the conditions in Table 2 for ¿ as a function of A at such bifurcations. We have included the cases $m D 0; 1$ for comparison, and also tabulate $!^2$, where $n 2 f0; 1; 2 : : :g$. Entries for $m > 3$ are straightforward but tedious to derive. In Figure 8, we plot f_2^n and f_3^n for $n D 0; 1$ and 2. Interestingly, f_2^0 has a vertical asymptote at $A D ¡8$, and f_3^0 has a vertical asymptote at $A D ¡4$. (It can be shown that these curves are not de□ned to the left of their asymptotes, since we require both ¿ and ! to be positive.)

Because of the nesting of the curves and

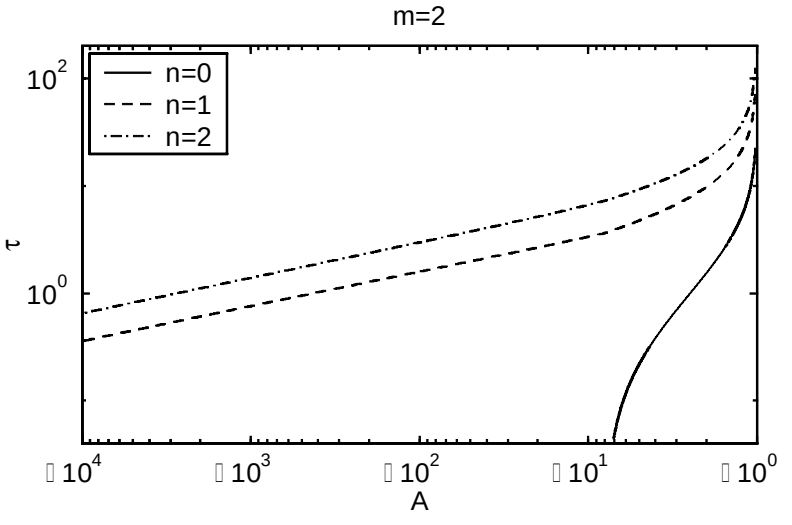
m=2
n=0
n=1
n=2
10^2
10^0
τ
10^4
10^3
10^2
10^1
10^0
A

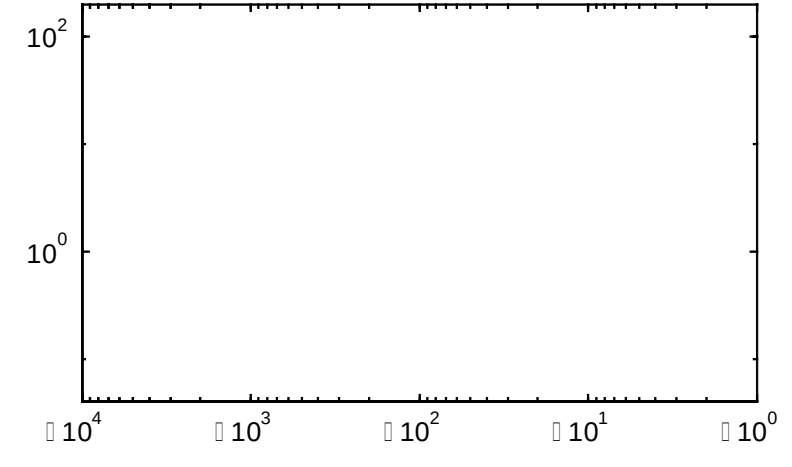
10^2
10^0
10^4
10^3
10^2
10^1
10^0

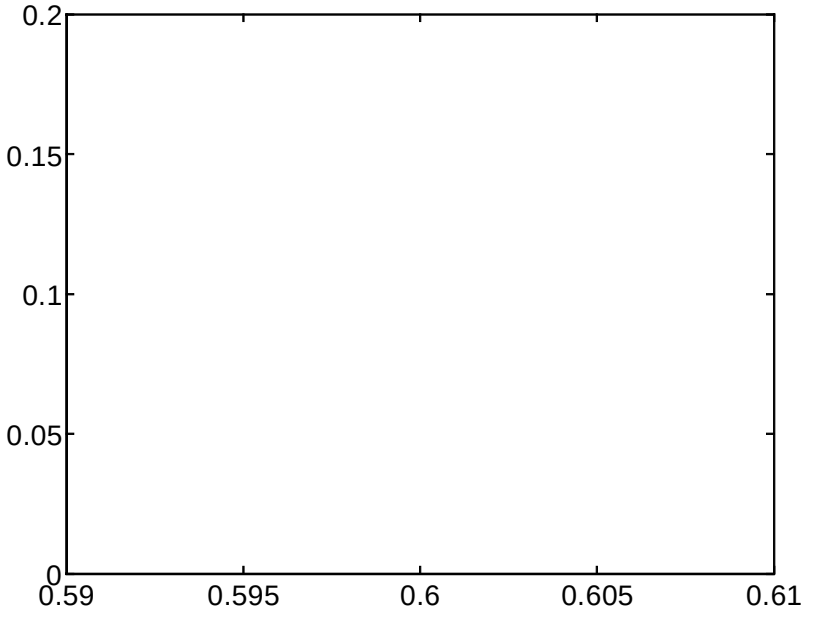
0.2
0.15
0.1
0.05
0
0.59
0.595
0.6
0.605
0.61

decreased. Note that at such a Hopf bifurcation, the frequency of oscillation is $! D a_i \sqrt{A^2 ¡ 1}$, so changing a_i will change the frequencies of oscillation.

In a similar way to that described in section 7.1, breaking the symmetry of $a_i D a_e$ breaks up the point $.I; Á/ D .0:6; 0:8667/$ in Figure 5 into a set of lower codimension points. For the case $a_i D 5$, $a_e D 1$, $¿_i D ¿_e D 1$, $¯ D 1$, $Á D 0:88$, a plot of frequency as a function of I is qualitatively the

points (not shown), we do not expect that any further breaking of symmetries (e.g., simultaneously having $\epsilon_i \neq \epsilon_e$ and $a_i \neq a_e$) would introduce any more novel behavior; rather, it would just move these points around in the $I; A$ plane. These codimension 2 points could be analyzed in detail by linearizing the appropriate systems about fixed points and investigating their stability.

8 Stochastic Paired Delayed Feedback

The analysis until now has been in the deterministic case, where there is a well-defined threshold for periodic firing in equation 2.2. However, noise is ubiquitous in neural systems, mainly as a result of the probabilistic nature of synaptic transmission (Koch, 1999). It is well known that including stochastic effects in single-neuron models "smoothes out" the abrupt change in slope of the frequency versus input current relationship that is seen in type I neurons (Hohn & Burkitt, 2001; Lansky & Sacerdote, 2001), of which the integrate–and–fire neuron we have studied is an example. How does this smoothing change the dynamics of the neuron with paired delayed feedback described up to now? This is a very broad and difficult question, especially since there are a number of ways to include noise such as synaptic noise in neuron models, and there are very few results in the literature on noise-driven systems with memory. The main difficulty in analyzing such systems stems from the non-Markovian nature of the problem, which precludes the use of standard tools such as Fokker-Planck analysis and the (related) first passage time to threshold calculations (Guillouzic, L'Heureux, & Longtin, 2000).

In this section, we approach this problem in a simple way, in the hope that the results will capture the essential effects of noise and, in particular, its smoothing of the firing function. We investigate the effects of noise of the leaky integrate-and-fire neuron with delayed feedback under study up to now by adding a stochastic term, $\sigma\xi(t)$, to equation 2.1, where $\xi(t)$ is gaussian white noise with zero mean and variance 1. The parameter σ adjusts the noise intensity. The firing rate of the neuron 2.1 is now given by (Ricciardi, 1977; Wang, 1999)

$$f = \left[\tau_r + \tau\sqrt{\pi}\int_{\frac{\epsilon-\mu}{\sigma}}^{\frac{\theta-\mu}{\sigma}} e^{u^2}\left(1+\operatorname{erf}(u)\right)du\right]^{-1},$$

and the error function is de□ned as erf.x/ D $^{2de\square}$

8.1 Numerical Implementation. We brie□y discuss the

8.4 Paired Feedback. When noise is added to the system, the point at $(I, A) = (0.6, 0.8667)$ in figure 5 breaks up. For small noise intensity, the curve of Hopf bifurcations in that figure, together with the line $I = 0.6$ for $0 < A < 0.8667$, forms a \-shaped curve, emanating from the I-axis. The Hopf bifurcation on the right side of this curve may be subcritical over some of its extent, depending on the values of α and $\bar{\ }$ (not shown).

The curve of saddle–node bifurcations of fixed points in Figure 5, together with the line $I = 0.6$ for $0.8667 < A < 1$, form a cusp emanating from the line $A = 1$. Thus, when $\alpha \neq 0$, there is an interval of A values (rather than just one value, as was the case for $\alpha = 0$) over which the feedback is "balanced," in the sense that it causes neither bistability not oscillations in frequency.

8.5 General Remarks. Adding noise does not destroy the chaotic behavior shown in section 4.3.1 (results not shown). This is to be expected, since the unimodal function shown in Figure 6 will not be destroyed by noise, merely smoothed out and shifted a little. In general, the effect of noise is to smooth out the discontinuity in the derivative of the firing function f and to put an upper bound on the absolute value of the derivative of this function. The effects of this on the existence and stability of fixed

potentials. Thus, the model properly treats the inherent time-dependent variations of the membrane time constant.

The model is also realistic in that it takes into account a possible minimal delay for the feedback, as well as the distribution of delays added to this minimal delay. This distribution characterizes the temporal spread of the feedback, that is, the distributed memory in the neural loop. The kernels for both feedback pathways can be used to model either direct feedback of the neuron onto itself or, alternately, feedback via one or more other neuron populations. Physiological data can then be used to fit the delay distributions and the feedback strengths (see, e.g., Mackey & an der Heiden, 1982; Berman & Maler, 1999; Eurich et al., 2002) and incorporate them into the model.

For excitatory feedback alone, our analysis revealed that the system can be quiescent, or fire periodically, or exhibit bistability between these two states. Inhibition alone produces quiescence, oscillatory firing rates, or bistability between constant and oscillatory firing-rate solutions. This means, for example, that an external input from, say, an afferent pathway can toggle the neural loop between periodic firing at a constant frequency and an oscillatory firing rate. Under certain conditions, this rate

deterministic □ring function. We □nd here that the smoothing provided by the noise removes the degeneracy in the deterministic function at □ring threshold, where the function is not differentiable. Adding noise puts an upper bound on the absolute value of the slope of this function, affecting the stability of □xed points of the system.

Signi□cant dynamical differences arise as the in□nite slope of the □ring function at oscillation onset becomes □nite, and the oscillation onset itself is smoothed out by the noise. For example, the oscillation in the □ring rate at the onset of □ring in the inhibitory case gives way to a constant □ring rate if noise is assumed (see Figure 11). Also, the noise can decrease and even annihilate the range of input currents where bistability occurs in the excitatory case.

Such

Bressloff, P. C., & Coombes, S. (2000b). A dynamical theory of spike train transitions in networks of integrate-and-□re oscillators. SIAM J. Appl. Math., 60, 820–841.

Brunel, N. (1996). Hebbian learning of context in recurrent neural networks. Neural Comput., 8, 1677–1710.

Cajal, R. S. (1909). Histologie du système nerveux de l'homme et des vertèbres. Paris: Maloine.

Campbell, S. A. (1999). Stability and bifurcation in the harmonic oscillator with multiple, delayed feedback loops. Dynam. Contin. Discrete Impuls. Systems, 5, 225–235.

Contreras, D., Destexhe, A., Sejnowski, T. J., & Steriade, M. (1996). Control of spatiotemporal coherence of a thalamic oscillation by corticothalamic feedback. Science, 274, 771–774.

Crick, F., & Koch, C. (1998). Constraints on cortical and thalamic projections: The no-strong-loops hypothesis. Nature, 391, 245–250.

Dayan, P., & Abbott, L.F. (2001). Theoretical neuroscience. Cambridge, MA: MIT Press.

Destexhe, A. (1994). Oscillations, complex spatiotemporal behavior, and information transport in networks of excitatory and inhibitory neurons.

Foss, J., Longtin, A., Mensour, B., & Milton, J. G. (1996). Phys. Rev. Lett., 76, 708–711.
Foss, J., & Milton, J. G. (2000). Multistability in recurrent neural loops arising from delay. J. Neurophysiol., 84, 975–985.
Giannakopoulos, F., & Zapp, A. (2001). Bifurcations in a planar system of differential delay equations modeling neural activity. Physica D, 159, 215–232.
Glass, L., & Mackey, M. C. (1988). From clocks to chaos: The rhythms of life. Princeton, NJ: Princeton University Press.
Glass, L., & Malta, C. P. (1990). Chaos in multilooped negative feedback systems. J. Theor. Biol., 145, 217–223.
Golomb, D., & Ermentrout, G. B. (2002). Slow excitation supports propagation of slow pulses in networks of excitatory and inhibitory populations. Phys. Rev. E, 65, 061911.
Guglielmi, N., & Hairer, E. (1999) Order stars and stability for delay differential equations. Numer. Math., 83, 371–383.
Guillouzic, S., L'Heureux, I., & Longtin, A. (2000). Rate processes in a delayed, stochastically driven, overdamped system. Phys. Rev. E, 61, 4906–4914.
Hahnloser, R. H. R., Sarpeshkar, R., Mahowald, M. A., Douglas, R. J., & Seung, H. S. (2000). Digital selection and analogue amplification in a cortex-inspired silicon circuit. Nature, 405, 947–951.
Hansel, D., & Mato, G. (2001). Existence and stability of persistent states in large neuronal networks. Phys. Rev. Lett., 86, 4175–4178.
Hansel, D., & Sompolinsky, H. (1992). Synchronization and computation in a chaotic neural network. Phys. Rev. Lett., 68, 718–721.
Hayes, N. D. (1950). Roots of the transcendental equation associated with a certain differential-difference equation. J. London Math. Soc., 25, 226–232.
Herz, A.V.M., Li, Z., & van Hemmen, J. L. (1991). Statistical mechanics of temporal association in neural networks with transmission delays. Phys. Rev. Lett., 66, 1370–1373.
Hohn, N., & Burkitt, A. N. (2001). Shot noise in the leaky integrate-and-fire neuron. Phys. Rev. E, 63, 031902.
Kistler, W.M. and van Hemmen, J.L. (1999). Delayed reverberation through time windows as a key to cerebellar function. Biol. Cybern., 81, 373–380.
Knight, B. W. (2000). Dynamics of encoding in neuron populations: Some general mathematical features. Neural Comput., 12, 473–518.
Koch, C. (1999). Biophysics of computation. New York: Oxford University Press.
Kunysz, A. M., Shrier, A., & Glass, L. (1997). Bursting behavior during fixed–delay stimulation of spontaneously beating chick heart cell aggregates. Am. J. Physiol., 273, C331–C346.
Lansky, P., & Sacerdote, L. (2001). The Ornstein-Uhlenbeck neuronal model with signal-dependent noise. Phys. Lett. A, 285, 132–140.
Latham, P. E., Richmond, B. J., Nelson, P. G., & Nirenberg, S. (2000). Intrinsic dynamics in neuronal networks. I. Theory. J. Neurophysiol., 83, 808–827.
Longtin, A., & Milton, J. G. (1988). Complex oscillations in the human pupil light reflex with mixed delayed feedback. Math. Biosc., 90, 184–199.